# Kinetics studies and oxide characterization in the internal oxidation of *Ag*In alloys

J. Desimoni, A. G. Bibiloni, L. Mendoza-Zélis, A. F. Pasquevich, F. H. Sánchez, and A. López-García
*Departamento de Física, Facultad de Ciencias Exactas,*
*Universidad Nacional de La Plata, 1900 La Plata, Argentina*
(Received 16 March 1983)

The internal oxidation of *Ag*In alloys has been investigated by time-differential perturbed angular correlation technique on $^{111}$In probes. We studied the oxidation kinetics of dilute (a few ppm) *Ag*In alloys at 300 °C under different annealing conditions and 1 at. % indium alloys at 300 °C and 550 °C. In some cases, the time dependence of the oxidation-front advance was ruled by a power law with an exponent different from 0.5. We determined the hyperfine parameters of $In_2O_3$ and studied the influence of the oxidation temperature on the indium sesquioxide precipitation in the silver matrix. A consistent description of the oxides formed at different temperatures is given.

## I. INTRODUCTION

Under certain conditions of concentration, oxygen pressure, and temperature, metal alloys based on a noble-metal solvent with a non-noble-metal solute undergo internal oxidation processes, i.e., oxidized solute particles appear in the noble-metal matrix. This leads to an oxidized rim whose border, called the oxidation front, progresses in depth as the oxidation proceeds. The internal oxidation process, particularly the oxidation kinetics, has been extensively studied mainly by microscopy. Recently we have applied time-differential perturbed angular correlations (TDPAC) to study this kind of phenomena.[1,2] The major advantage of this technique is its sensitivity to the charge distribution in the neighborhood of the ion probe through the quadrupole hyperfine interaction, being in this way capable of distinguishing the different probe-oxygen configurations. If the hyperfine parameters that characterize a given oxide were known, then its presence in the studied matrix could be recognized.

We have already shown that the system *Ag*In is appropriate to internal oxidation studies.[1] In previous work we dealt with very diluted alloys whose oxidation led to several configurations of Ag-In-O complexes, evidenced by the presence of a rather broadly distributed interaction. However, we found that the concept of a sharp oxidation front remains valid, the oxidation kinetics at 400 °C and 500 °C being well described by a parabolic law.[2] In these studies, the low indium concentration, compared with those of other oxidizable impurities present in the matrix, precludes the determination of the average composition of the indium oxides formed.

In the present work, in addition to an extension to lower temperatures (300 °C) of the TDPAC studies of dilute *Ag*In alloys, we performed experiments on *Ag*In alloys of definite concentration, namely 1 at. % In, with the aim of studying its oxidation kinetics as well as characterizing the resulting oxides. This concentration was chosen in the hope that it was sufficiently large to produce the formation of oxide precipitates with a well-defined composition. The TDPAC measurements were done on alloys that had different previous treatments, were oxidized at various temperatures, and followed several sequences of annealings for the purpose of studying the conditions for the formation of a given oxidized compound and its stability.

In order to understand the obtained results, complementary measurements were performed on alloys with 4 and 7 at. % In. For these concentrations, x-ray determinations by Dietrich and Koch[3] revealed the presence of $In_2O_3$ precipitates. On the other hand, we studied the hyperfine interactions in chemically prepared $In_2O_3$. These experiments might also show if there is any influence of the silver matrix on the structure of the oxides.

The results presented here allow a characterization of the $In_2O_3$ hyperfine parameters and detection of $In_2O_3$ in the silver matrix as well as a reasonable description of the internal oxidation processes that occur, depending on the oxidation temperatures. Recent results of Wodniecki and Wodniecka[4] concerning *Ag*In alloys at concentrations lower than 1 at. % In are also discussed in connection with ours.

## II. EXPERIMENTAL

The $^{111}$Cd obtained from the decay of $^{111}$In ($\tau$=2.81 d) was used for the TDPAC measurements. The $^{111}$In activity was produced by the reaction $^{109}$Ag($\alpha$,2$n$)$^{111}$In on silver foils (99.99% purity) with 56-MeV $\alpha$ particles. The minor influence of other activities that were also produced was discussed elsewhere.[2] The $^{111}$In concentration always remained below 10 ppm. The alloys were prepared by melting the irradiated silver foils together with appropriate amounts of inactive high-purity indium metal in quartz capsules filled with Ar at a pressure of 120 mm Hg. Afterward, the samples were rolled down to their final thickness and, in some cases, thermally annealed at 800 °C in Ar and C for about 2 h. Then, TDPAC spectra were taken before any oxidation treatment.

The oxidation treatments were performed by heating the samples in silica tubes open to the air in a conventional electric oven, stable to within 4 °C, at the proper temperature. The kinetics of oxidation was followed by cumulative oxidation treatments on each sample. When the TDPAC measurements were made above room temperature a conventional electric heater, stable to within 5 °C, was used.

The measurements of the $In_2O_3$ were performed on powder doped with $^{111}$In prepared in the following way: A natural cadmiun foil was irradiated with 28-MeV deuterons and then dissolved in $HNO_3$ together with some indi-

 

um metal. Then, $H_2S$ was bubbled into the solution, and the yellow precipitate of CdS was eliminated by centrifugation. This process was repeated until no visible CdS was present. The solution was then evaporated, and the $In_2O_3$ was obtained by calcination of $In(NO_3)_3$ at about 500 °C. The suitability of the described process was checked by x-ray analysis of the resulting product, whose Debye-Scherrer pattern only showed the characteristic lines of $In_2O_3$ (80*B*) reported by Swanson, Gilfrich, and Ugrimic.[5]

A description of the electronic equipment and data analysis used for the TDPAC experiments can be found in Ref. 2. Experimental asymmetry ratios $R(t)$ were evaluated and fitted with theoretical functions of the form $A_2G_2(t)$ folded with the measured time-resolution curve (full width at half maximum of 2.4 ns). The proposed perturbation factors were of the form

$$G_2(t)=f_0+\sum_i f_i \sum_{n=0}^{3} s_{n,i}\exp(-\delta_i\omega_{n,i}t)\cos(\omega_{n,i}t) ,$$

where $f_i$ are the relative fractions of nuclei that experience a given perturbation and $f_0$ corresponds to unperturbed probes. The frequencies $\omega_n$ are related by $\omega_n=F_n(\eta)\omega_Q$ to the quadrupolar frequency $\omega_Q=eQV_{zz}2\pi/40h$. The coefficients $F_n$ and $s_n$ are known functions[6] of the axial asymmetry parameter $\eta$ defined by $\eta=(V_{xx}-V_{yy})/V_{zz}$. The exponential function accounts for a Lorentzian frequency distribution of relative width $\delta$ around $\omega_n$.

## III. RESULTS

For the kinetics at 300 °C three samples were used. Their thicknesses, concentrations, and previous thermal treatments are given in Table I. In Fig. 1, TDPAC spectra taken on sample 3 are shown, labeled according to the time of oxidation. In all these samples we found a quite broadly distributed electric quadrupole interaction, characterized by the parameters

$$\omega_Q=10 , \quad \eta=0.5 , \quad \delta=0.4 ,$$

with $\omega$ in MHz, that could be assigned to the oxidation of the probes. In the case of 1-at. % In alloys a low-frequency component ($\omega_Q\simeq 1$ MHz) associated with the loss of cubic symmetry of the matrix can also be seen. This interaction originated in the higher concentration range of indium, and it was found to be already present in the TDPAC spectra of the nonoxidized samples.

The TDPAC results for the kinetics at 550 °C (sample 4, see Fig. 2) show clearly the presence of two well-defined hyperfine interactions, whose typical parameters are

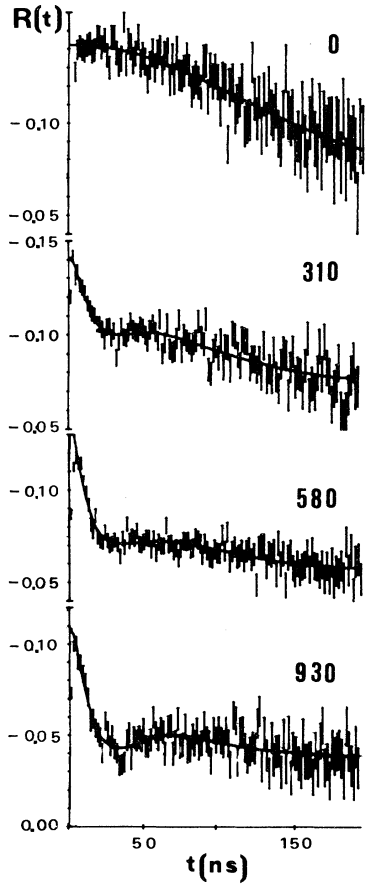


FIG. 1. TDPAC spectra after successive oxidation treatments at 300 °C of a 0.035-mm 1-at. % In sample preannealed at 700 °C for 30 min. All measurements were done at room temperature. The cumulative time of oxidation, in minutes, is indicated. Solid lines show the curves fitted to the data.

$$\omega_{Q_1}=18.5 , \quad \eta_1=0.75, \quad \delta_1=0.08 ,$$

$$\omega_{Q_2}=24.5, \quad \eta_2=0.22 , \quad \delta_2=0.04 ,$$

where $\omega$ is given in MHz. The amplitudes of these interactions are in a ratio $f_1:f_2$ of about 3:2. The low frequency of about 1 MHz is also present.

In Figs. 3 and 4, the evolution of the fraction $f$ of oxidized probes as a function of the duration $t$ of the oxidation process is shown. The expression

TABLE I. Characteristics of the four samples used for kinetics studies in this work. Thermal treatments are described. The exponent $m$ resulting from fits of expression (1) to the experimental data is also given.

| Sample | Indium concentration | Annealing treatment | Oxidation temperature (°C) | Thickness (mm) | $m$ |
|---|---|---|---|---|---|
| 1 | diluted | 70 min×800 °C | 300 | 0.290 | $0.61_2$ |
| 2 | diluted | | 300 | 0.165 | $0.88_4$ |
| 3 | 1 at. % | 30 min×700 °C | 300 | 0.035 | $0.74_{12}$ |
| 4 | 1 at. % | | 550 | 0.250 | $0.58_{11}$ |

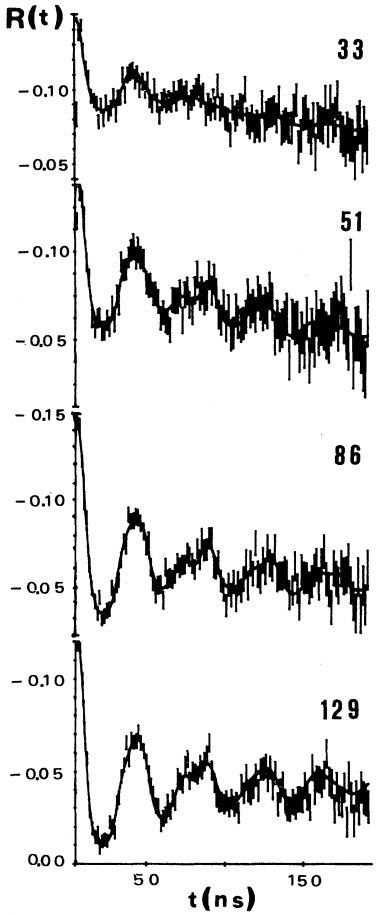


FIG. 2. TDPAC spectra after successive oxidation treatments at 550°C of a 0.250-mm 1-at.% In sample. All measurements were done at room temperature. The cumulative time of oxidation, in minutes, is indicated. Solid lines show the curves fitted to the data.

$$f = \text{const} \times t^m \quad (1)$$

was fitted to the experimental results, and the obtained $m$ values are shown in Table I. The fraction $f$ of oxidized probes is connected with the depth $\xi$ of the oxidation front by $f = 2\xi/d$, where $d$ is the sample thickness.

The presence of two well-defined interactions, when the oxidation is carried out at 550°C, suggests the existence of either two different oxides or one oxide with two inequivalent indium sites. We investigated the nature of these interactions as well as the temperature range in which they are established. For this purpose we performed TDPAC measurements (Fig. 5) on $In_2O_3$ prepared according to the method described in the preceding section. The result consists essentially of the same two interactions already found ($f_1 = 0.32$, $\omega_{Q_1} = 18.5_{1.0}$ MHz, $\eta_1 = 0.74_1$, $\delta_1 = 0.020_2$, and $f_2 = 0.16$, $\omega_{Q_2} = 24.5_{1.0}$ MHz, $\eta_2 = 0.11_4$, $\delta_2 = 0.010_2$) plus an important time-dependent perturbation contribution. In addition, these interactions were obtained from samples with 4 and 7 at.% In oxidized at 550°C (see also Fig. 5). Only the characteristic

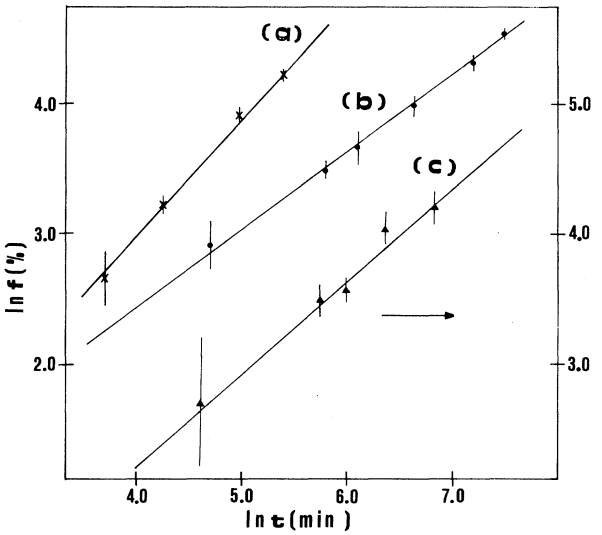


FIG. 3. Logarithmic plot showing the evolution of the fraction $f$ of oxidized probes ($T_{ox} = 300$°C) as a function of the time of oxidation: (a) sample 2, (b) sample 1, and (c) sample 3.

lines of $In_2O_3$ showed up in x-ray analyses performed on these samples.

In order to determine the necessary conditions for establishing these well-defined interactions, TDPAC measurements on 1-at.% alloys, oxidized at temperatures ranging from 300°C to 700°C, were performed. In Table II the results of a least-squares fit to these measurements are shown. As can be seen, the above-mentioned interactions of frequencies $\omega_{Q_1} = 18.5$ MHz and $\omega_{Q_2} = 24.5$ MHz appeared only at oxidation temperatures above 400°C, whereas a more distributed interaction of 18.5 MHz is already present at lower temperatures.

Further experiments showed that samples that had been oxidized at low temperatures ($T_{ox} \leq 400$°C) do not show the above-mentioned well-defined interactions when reoxidized at 500°C, but these two interactions clearly appear when reoxidized at very high temperatures or melted in Ar atmosphere.

In order to study the nature of the time-dependent interaction we performed measurements on $In_2O_3$ at 300°C

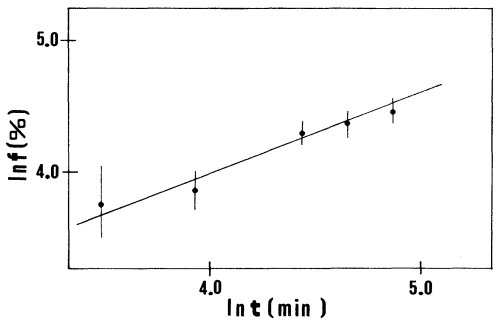


FIG. 4. Logarithmic plot showing the evolution of the fraction, $f$ of oxidized probes as a function of the time of oxidation, for sample 4, oxidized at 550°C.

TABLE II. Fitted values of the parameters characterizing the observed interactions. Quadrupolar frequencies $\omega_{Q_i}$ are given in MHz. Parameters associated with nonoxidized probes are omitted for simplicity.

| $T_{ox}$ (°C) | $f_1$ | $\omega_{Q_1}$ | $\eta_1$ | $\delta_1$ | $f_2$ | $\omega_{Q_2}$ | $\eta_2$ | $\delta_2$ | $f_3$ | $\omega_{Q_3}$ | $\eta_3$ | $\delta_3$ | $f_4$ | $\omega_{Q_4}$ | $\eta_4$ | $\delta_4$ |
|---|---|---|---|---|---|---|---|---|---|---|---|---|---|---|---|---|
| 300 | | | | | | | | | | | | | $0.68_7$ | $10.0_5$ | $0.55_{25}$ | $0.45_{14}$ |
| 350 | | | | | | | | | $0.44_{12}$ | $18.0_5$ | $0.62_4$ | $0.16_3$ | $0.55_{10}$ | $9.0_8$ | $0.49_{15}$ | $0.32_4$ |
| 400 | | | | | | | | | $0.91_9$ | $19.0_8$ | $0.54_6$ | $0.30_5$ | | | | |
| 450 | $0.27_{15}$ | $18.0_5$ | $0.80_5$ | $0.10_7$ | $0.10_3$ | $25.0_5$ | $0.15_6$ | $0.01_2$ | $0.63_{15}$ | $19_2$ | $0.52_{10}$ | $0.34_7$ | | | | |
| 500 | $0.53_{10}$ | $18.0_5$ | $0.69_5$ | $0.10_2$ | $0.44_{11}$ | $24.0_7$ | $0.30_9$ | $0.17_3$ | | | | | | | | |
| 550 | $0.50_6$ | $18.5_5$ | $0.77_2$ | $0.08_2$ | $0.37_6$ | $24.0_5$ | $0.22_3$ | $0.05_1$ | | | | | | | | |
| 700 | $0.64_4$ | $18.0_5$ | $0.73_1$ | $0.05_1$ | $0.32_4$ | $24.0_5$ | $0.22_2$ | $0.03_1$ | | | | | | | | |
| 1000 | $0.74_3$ | $18.0_5$ | $0.74_1$ | $0.04_1$ | $0.20_2$ | $24.0_5$ | $0.22_2$ | $0.01_1$ | | | | | | | | |

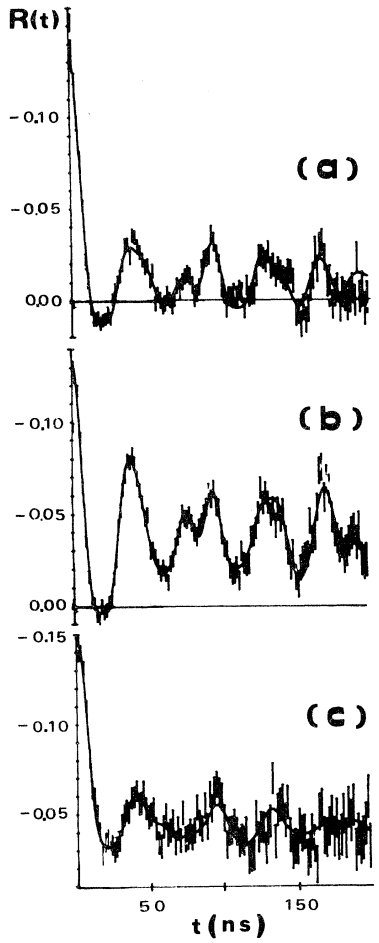


FIG. 5. TDPAC spectra at room temperature of (a) $In_2O_3$, (b) *Ag*In, 1-at. % alloy oxidized at 1000 °C, and (c) *Ag*In, 7-at. % In alloy oxidized at 550 °C.

and 550 °C (Fig. 6) and on oxidized 7-at. % alloys at 300 °C (Fig. 7). The results show primarily that the time-dependent perturbation gradually decreases with temperature. More information related to aftereffect phenomena to which it seems to be connected could be probably obtained. For this purpose further experiments are in progress and will be presented shortly.

## IV. DISCUSSION

The kinetic behavior of the internal oxidation at 300 °C was studied for three different cases: diluted alloys with and without previous annealings and 1-at. % In alloys with previous annealing. In all cases the hyperfine interaction parameters were similar. Therefore they could be attributed to the same Ag-In-O complexes. At this temperature the obtained $m$ values for samples 2 and 3 are clearly greater than the value of 0.5, which corresponds to a diffusion-controlled process with a constant effective diffusion coefficient. The exponent close to 1 obtained for sample 2 may be related to the lack of annealing previous to the oxidation, since an annealed sample (sample 1)

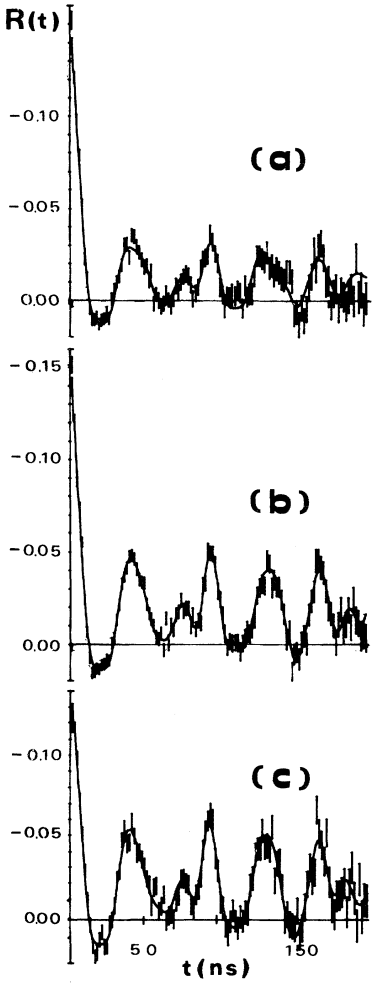


FIG. 6. TDPAC spectra of $In_2O_3$ measured at (a) room temperature, (b) 300 °C, and (c) 550 °C.

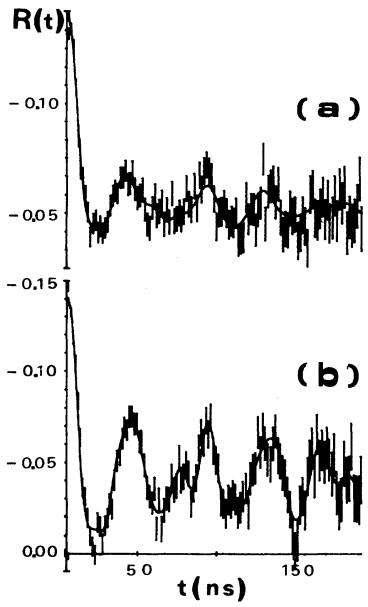


FIG. 7. TDPAC spectra of *Ag*In 7-at. % In alloy measured at (a) room temperature and (b) 300 °C.

shows a nearly parabolic kinetics. It is not clear yet how the fissures and other imperfections introduced by the cold work may affect the oxidation kinetics. In the case of sample 3 (1-at. % In alloy) this argument should not apply, and another mechanism must be invoked to explain the observed kinetics. The high concentration of isolated, internally oxidized indium atoms could produce an inhomogeneous strain field that enhances the oxygen diffusion through short-circuit diffusion paths. These strain fields were observed by Huffman and Podgurski[7] in *Ag*Sn 0.33-at. % Sn alloys.

The kinetics at the rather high temperature of 550 °C, sample 4, has a behavior close to a parabolic time dependence of the progress of the internal oxidation front (see Fig. 4). Here, we expect that the lack of previous annealing becomes less important due to the recovering produced by the oxidation treatment itself. Furthermore, it seems that the oxidation process does not introduce a noticeable number of short-circuit diffusion paths in this case, probably indicating that there is nucleation of oxidized indium atoms. This difference in the oxide structures, depending on the oxidation temperature, is clearly manifest in the measured hyperfine interactions.

In order to discuss the nature of these oxides let us consider the results we obtained with $In_2O_3$ chemically prepared. The two static interactions that we found in this compound at room temperature must be associated with two inequivalent indium sites in the oxide, in agreement with the two sites reported in the literature.[8] Indeed, the unit cell of the $In_2O_3$ that belongs to the bixbyite-type $T_h^7(Ia_3)$ space group has 16 molecules, with two different indium sites *d* and *a* with relative populations 3:1. Essentially, this structure consists of In ions coordinated by six O ions in two different geometries. The symmetry of these sites is such that, from point-charge calculations, an axially symmetric electric field gradient (EFG) is expected for site *a* and an asymmetric EFG ($\eta=0.7$) for site *d*. The same calculations lead to $V_{zz}^a/V_{zz}^d \simeq 2$. Therefore we ascribed the more intense interaction ($\omega_{Q_1}=18.5$ MHz, $\eta_1=0.74$) to site *d* and the other interaction ($\omega_{Q_2}=24.5$ MHz, $\eta_2=0.11$) to site *a*, although their measured relative amplitude ratio is 2:1. This discrepancy could be correlated with the existence of a fraction of nuclei that experience a time-dependent interaction if both sites contributed in a different extent to this interaction. Support to this argument is given by the measurements at high temperatures, 300 °C and 550 °C, where the amplitude of the time-dependent interaction decreases, and the ratio between the static interactions tends gradually to 3:1.

Earlier TDPAC measurements of Salomon[9] on indium sesquioxide also show an admixture of a static perturbation and a time-dependent perturbation even though the oxide was prepared in a different way. The overall aspect of his TDPAC pattern is similar to ours, but a distinction between two different indium sites is masked by the reduced time range that he observed (50 ns).

Comparing the results for $\omega$, $\eta$, and $\delta$ obtained in our experiments of internal oxidation in 1-at. % In alloys (see

Table II) with those of $In_2O_3$, it is clear that at oxidation temperatures above 450 °C precipitates of this oxide are formed. A dispersion in the ratio $f_1:f_2$ and a deviation from the expected value are observable. Anyway, it is possible to fix the ratio $f_1:f_2$ at the ideal value of 3 without any significant loss in the quality of the fit and also without change in the parameters that define the two observed interactions or in the total amplitude $f_1+f_2$.

At this point we would like to comment on recent TDPAC results of Wodniecki and Wodniecka.[4] They studied the internal oxidation of the *Ag*In system at concentrations $c \leq 0.5$ at. % In and also found, for oxidation temperatures above 500 °C, two well-defined interactions of 18.3 and 24.6 MHz, but these were ascribed to two different kind of oxides. While this assignment is inconsistent with the existence of two different lattice sites in the $In_2O_3$ structure, their experimental results support our interpretation. In effect, above 600 °C the reported amplitudes for the mentioned 18.3- and 24.6-MHz interactions are in good agreement with the 3:1 ratio expected for the relative site populations in $In_2O_3$ precipitates.

We can now interpret all the interactions we observed according to the following mechanism of oxide formation.

(a) The interaction of 10 MHz, predominant at $T_{ox}=300$ °C and gradually decreasing with increasing temperatures (see Fig. 8), can be assigned to the oxidation of isolated atoms since the parameters that characterize this interaction are similar to those already observed in diluted alloys.[2]

(b) The interaction of $\omega_Q=18.5$ MHz, $\eta=0.60$ that appears at oxidation temperatures between 350 °C and 450 °C should not be ascribed to $In_2O_3$ precipitates due to the absence of the 24.5-MHz interaction. In addition, this interaction is much more broadly distributed than the interaction that appears in $In_2O_3$. We think that it can be assigned to clusters of oxidized indium. Nevertheless, it seems that the similarity between these parameters and those of site *d* in $In_2O_3$ is not mere coincidence. We think that these clusters, where the In ions are probably sixfold coordinated, are the origin of the indium sesquioxide.

(c) The two well-defined interactions of $\omega_{Q_1}=18.5$ MHz, $\eta_1=0.74$, $\delta_1=0.08$ and $\omega_{Q_2}=24.5$ MHz, $\eta_2=0.22$, $\delta_2=0.04$ that appear at $T_{ox} \geq 450$ °C correspond, as discussed above, to $In_2O_3$ precipitates.

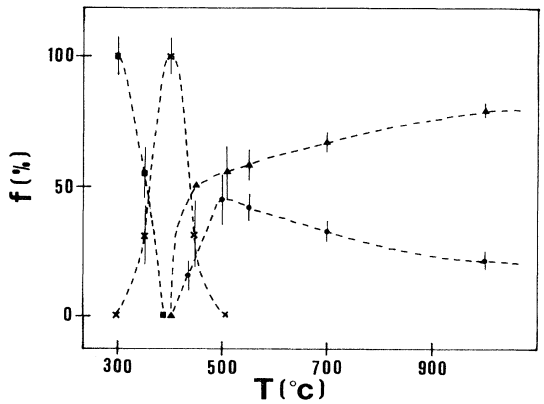


FIG. 8. Relative amplitudes of the individual hyperfine interactions observed at different oxidation temperatures. ■: $\omega_Q=10$ MHz, $\eta\simeq0.5$. ×: $\omega_Q=18.5$ MHz, $\eta\simeq0.6$. ▲; $\omega_Q=18.5$ MHz, $\eta\simeq0.74$. ●: $\omega_Q=24.5$ MHz, $\eta\simeq0.22$.

This interpretation is consistent with simple theoretical predictions[10] about the relative size of precipitates formed at different temperatures of oxidation. For *Ag*In alloys the precipitates formed at 500 °C are 15 times larger than those formed at 400 °C. Therefore we can expect the precipitate size will enlarge, tending to the proper crystal structure of $In_2O_3$ when the oxidation temperature is increased. This interpretation accounts for the quasiparabolic kinetics observed at 550 °C, since in this case the oxidized zone consists mainly of precipitates, about 40 000 times larger than those formed at 300 °C, in a nearly undistorted silver matrix.

It should be noted that the results of Wodniecki and Wodniecka on 0.5-at. % alloys reveal sesquioxide precipitation for $T_{ox} \geq 500$ °C instead of 450 °C in this work. This difference can be accounted for by the different indium concentrations involved. Calculations similar to those referred to above predict that precipitates of the same average size form at 500 °C in 0.5-at. % alloys and at 450 °C in 1-at. % alloys for the involved sample thicknesses.

The composition of the oxides formed at a given temperature can also be extracted from a parabolic kinetics result. If we plot the fraction of oxidized probes versus $t^{1/2}$, a straight line can be fitted. Its slope depends on the temperature, sample thickness, solute concentration, and the number $\nu$ of oxygen atoms per solute atom in the oxide. Applying Wagner's theory, outlined in Ref. 2, we obtain from the 550 °C kinetics results $\nu=1.3$. This result is in good agreement with the expected value for $In_2O_3$. In effect, $In_2O_3$ is a compound whose stoichiometry depends on the preparation method, and the [O]/[In] ratio is generally lower than 1.5.

From the results of the reoxidation experiments reported in the preceding section it is clear that $In_2O_3$ precipitation will not occur at 500 °C if the sample has been previously fully oxidized at low temperature ($T_{ox} \leq 400$ °C). Obviously this is connected with the stability of the low-temperature complexes. However, when the reoxidation temperature is sufficiently high (900 °C) these complexes decompose, allowing indium migration to form $In_2O_3$. This internal oxide does not decompose under annealing at 900 °C in a reducing atmosphere.

## V. CONCLUSIONS

At oxidation temperatures of 300 °C a quasiparabolic kinetics is observed in dilute preannealed alloys. When the solute concentration is increased (1 at. % In) a deviation from this behavior is observed and tentatively attributed to the existence of short-circuit diffusion paths created by the oxidation process. When the oxide precipitation is favored ($T_{ox}=550$ °C) an almost parabolic kinetics is found again.

Depending on the oxidation temperature and alloy composition different kinds of internal oxides are detected in the silver matrix, ranging from isolated oxidized In atoms to $In_2O_3$ precipitates.

Finally, the possibility of having $In_2O_3$ precipitates of variable size embedded in a highly conducting metallic environment could be useful in understanding the observed

time-dependent perturbation and its possible connection with aftereffect phenomena.

## ACKNOWLEDGMENTS

The authors acknowledge the cooperation of Dr. G. Punte and H. R. Viturro, Laboratorio de Rayos X, Departamento de Física, in making the x-ray analyses and to the staff of the Comisión Nacional de Energía Atómica (CNEA), Argentina, for irradiation facilities. The authors are also grateful to Consejo Nacional de Investigaciones Científicas y Técnicas (CONICET), Comisión de Investigaciones Científicas de la Provincia de Buenos Aires (CICPBA), and Subsecretaría de Ciencia y Técnica (SUBCYT), Argentina, and Kernforschungszentrum Karlsruhe GmbH, West Germany, for partial economic support.

[1]A. F. Pasquevich, A. G. Bibiloni, C. P. Massolo, F. H. Sánchez, and A. López-García, Phys. Lett. 82A, 34 (1981).

[2]A. F. Pasquevich, F. H. Sánchez, A. G. Bibiloni, J. Desimoni, and A. López-García, Phys. Rev. B 27, 963 (1983).

[3]I. Dietrich and L. Koch, Z. Metallkd. 50, 31 (1959).

[4]P. Wodniecki and B. Wodniecka, Hyperfine Interact. 12, 95 (1982).

[5]H. E. Swanson, N. T. Gilfrich, and G. M. Ugrimic, NBS Circular 539 (U.S. GPO, Washington, D.C., 1955), Vol. 5, p. 27.

[6]L. A. Mendoza-Zélis, A. G. Bibiloni, M. C. Caracoche, A. López-García, J. A. Martínez, R. C. Mercader, and A. F. Pasquevich, Hyperfine Interact. 3, 315 (1977)).

[7]G. P. Huffman and H. H. Podgurski, Acta Metall. 21, 449 (1973).

[8]R. W. G. Wyckoff, in *Crystal Structures* (Interscience, New York, 1968), Vol. II, p. 4; M. Marezio, Acta Crystallogr. 20, 723 (1966).

[9]M. Salomon, Nucl. Phys. 54, 171 (1964).

[10]F. H. Sánchez, R. C. Mercader, A. F. Pasquevich, A. G. Bibiloni and A. López-García (unpublished).